OXFORD

SOT | Society of Toxicology
www.toxsci.oxfordjournals.org

TOXICOLOGICAL SCIENCES, 150(2), 2016, 488–498

doi: 10.1093/toxsci/kfw015
Advance Access Publication Date: January 21, 2016
Research Article

MMP-9-Dependent Serum-Borne Bioactivity Caused by Multiwalled Carbon Nanotube Exposure Induces Vascular Dysfunction via the CD36 Scavenger Receptor

Mario Aragon,* Aaron Erdely,† Lindsey Bishop,† Rebecca Salmen,† John Weaver,* Jim Liu,* Pamela Hall,* Tracy Eye,† Vamsi Kodali,† Patti Zeidler-Erdely,† Jillian E. Stafflinger,‡ Andrew K. Ottens,‡ and Matthew J. Campen*,[1]

*Department of Pharmaceutical Sciences, University of New Mexico College of Pharmacy, Albuquerque, New Mexico 87131; †National Institute for Occupational Safety and Health, Morgantown, West Virginia 26508; and ‡Department of Anatomy and Neurobiology, Virginia Commonwealth University School of Medicine, Richmond, Virginia 23298

[1]To whom correspondence should be addressed at Department of Pharmaceutical Sciences, University of New Mexico, Albuquerque, NM 87131. Fax: (505) 925-7778. E-mail: mcampen@unm.edu.

ABSTRACT

Inhalation of multiwalled carbon nanotubes (MWCNT) causes systemic effects including vascular inflammation, endothelial dysfunction, and acute phase protein expression. MWCNTs translocate only minimally beyond the lungs, thus cardiovascular effects thereof may be caused by generation of secondary biomolecular factors from MWCNT-pulmonary interactions that spill over into the systemic circulation. Therefore, we hypothesized that induced matrix metalloproteinase-9 (MMP-9) is a generator of factors that, in turn, drive vascular effects through ligand-receptor interactions with the multiligand pattern recognition receptor, CD36. To test this, wildtype (WT; C57BL/6) and MMP-9$^{-/-}$ mice were exposed to varying doses (10 or 40 μg) of MWCNTs via oropharyngeal aspiration and serum was collected at 4 and 24 h postexposure. Endothelial cells treated with serum from MWCNT-exposed WT mice exhibited significantly reduced nitric oxide (NO) generation, as measured by electron paramagnetic resonance, an effect that was independent of NO scavenging. Serum from MWCNT-exposed WT mice inhibited acetylcholine (ACh)-mediated relaxation of aortic rings at both time points. Absence of CD36 on the aortic rings (obtained from CD36-deficient mice) abolished the serum-induced impairment of vasorelaxation. MWCNT exposure induced MMP-9 protein levels in both bronchoalveolar lavage and whole lung lysates. Serum from MMP-9$^{-/-}$ mice exposed to MWCNT did not diminish the magnitude of vasorelaxation in naïve WT aortic rings, although a modest right shift of the ACh dose–response curve was observed in both MWCNT dose groups relative to controls. In conclusion, pulmonary exposure to MWCNT leads to elevated MMP-9 levels and MMP-9-dependent generation of circulating bioactive factors that promote endothelial dysfunction and decreased NO bioavailability via interaction with vascular CD36.

Key words: carbon nanoparticle; vascular; cardiovascular; toxicity; serum; CD36; MMP-9.

Pulmonary exposure to nanomaterials such as carbon nanotubes is associated with the progression of cardiovascular disease in vulnerable animal models (Li *et al.*, 2007). However, gaps exist in our understanding of the pathways by which inhaled substances affect the systemic vasculature, and this hinders our ability to predict risk and identify potentially vulnerable

subpopulations. Inhaled nanomaterials, such as multiwalled carbon nanotubes (MWCNTs), have limited ability to translocate into the systemic circulation (Mercer *et al.*, 2013) and evidence for a direct interaction between nanomaterials and vascular cells at relevant exposure concentrations is lacking. Several studies have demonstrated more profound systemic vascular effects arising from particle inhalation (Nurkiewicz *et al.*, 2008, 2009; Sun *et al.*, 2005) as compared with gavage or even direct intravenous injection (Bai *et al.*, 2007; Folkmann *et al.*, 2012), suggesting that secondary, circulating factors induced by pulmonary responses to exposure contribute to adverse cardiovascular effects.

Central to the development of cardiovascular disease is the activation of the endothelium, characterized by the increased expression of adhesion molecules, extravasation of leukocytes, and the loss of endothelial nitric oxide synthase (eNOS) function (Aird, 2008). eNOS produces the diffusible molecule nitric oxide (NO), which is anti-inflammatory, anti-coagulatory, and vasodilatory (Alheid *et al.*, 1987; Kubes *et al.*, 1991; Nunokawa and Tanaka, 1992). In an atherosclerotic state, eNOS becomes "uncoupled" leading to the loss of NO bioavailability (Harrison, 1994). Loss of NO enhances the proinflammatory environment that is central to the progression of atherosclerosis. Mounting evidence suggests that pattern recognition (eg, Toll-like receptor-4, aka TLR4) and/or scavenger receptors (eg, CD36) play a prominent role in mediating endothelial activation (Shaul, 2003; Wang *et al.*, 2011). Lipid peroxidation products present in the lung lining fluid following exposure to particulate matter (PM) mediate systemic cellular inflammatory responses through TLR4, and such modified lipids have been shown to be present following exposure to concentrated ambient PM (Kampfrath *et al.*, 2011). CD36, a class B scavenger receptor, recognizes many ligands, such as thrombospondin and oxidized low density lipoprotein (LDL) cholesterol, and is widely expressed on the surface of multiple cell types, including macrophages and endothelial cells (Febbraio *et al.*, 1999; Sawada *et al.*, 2012). CD36 is involved in atherosclerosis and inflammation (Febbraio *et al.*, 2001) and is required for the endothelial dysfunction induced by inhalation to the reactive gas ozone (Robertson *et al.*, 2013).

One potential source of circulating ligands that interact with pattern recognition receptors following inhalation exposure is activation of matrix metalloproteinases (MMPs) in the lung (Su *et al.*, 2000). MMPs have been shown to be involved in a wide range of process including development, wound healing, and host defense (Dagouassat *et al.*, 2012). MMP-9, an MMP that binds collagen-based substrates, has been shown to be unregulated and activated following exposure to PM and PM-containing combustion mixtures (Lund *et al.*, 2009, 2011; Su *et al.*, 2000). Erdely *et al.* (2009) reported increased gene expression of MMP-9 in the lung, as well as an increase in circulating MMP-9 as a result of pulmonary MWCNT-7 exposure. The pathophysiological relevance of MMP-9 activation following pulmonary exposure to nanomaterials remains unknown.

Currently, no studies exist investigating the potential links between vascular dysfunction, MMPs, CD36, and nanomaterial exposure. We hypothesized that MWCNT-7 exposure activates MMPs in the lung, leading to the generation of circulating ligands that may directly impact vascular function through the CD36 receptor. To test this hypothesis, we applied an innovative *ex vivo* methodology for assessing potential cumulative effects of circulating mediators on vascular function. In this study, we demonstrated that MWCNT-7 exposure induces the generation of circulating bioactive factors that diminish stimulated NO production and impair vasorelaxation in a manner that is dependent on MMP-9 and vascular CD36.

MATERIALS AND METHODS

Animals

Specific pathogen-free, male C57BL/6J and MMP-9$^{-/-}$ (B6.FVB(Cg)-Mmp9^{tm1Tvu}/J) mice from Jackson Laboratory (Bar Harbor, ME) and CD36$^{-/-}$ mice on a C57BL/6 background, bred in-house (obtained from Mario Febbraio), were used in this study. C57BL/6J and MMP-9$^{-/-}$ mice for exposures were housed in the AAALAC-approved NIOSH Animal Facility, while naïve mice (C57BL/6J and CD36$^{-/-}$) for donating aortas were housed in AAALAC-approved facilities at the University of New Mexico. All mice were provided food and tap water *ad libitum* in ventilated cages in a controlled humidity and temperature environment with a 12 h light/dark cycle. Animal care and use procedures were conducted in accordance with the "PHS Policy on Humane Care and Use of Laboratory Animals" and the "Guide for the Care and Use of Laboratory Animals" (NIH publication 86-23, 1996). These procedures were approved by the respective Institutional Animal Care and Use Committees of the National Institute for Occupational Safety and Health and the University of New Mexico.

Mice, 8 weeks of age, were treated via oropharyngeal aspiration with MWCNT (MWNCT-7/Mitsui-7) at 0, 10, or 40 μg (n = 12 for each group was needed to generate enough serum for all tests) in a volume of 50 μl. The MWCNT were prepared in a physiologic dosing media (DM) for the vehicle that consisted of mouse serum albumin (0.6 mg/ml) and 1,2-dipalmitoyl-sn-glycero-3-phosphocholine (10 μg/ml) in phosphate-buffered saline (PBS), with sonication for 5 min to ensure dispersion. The MWCNT used in this study, MWCNT-7, have been extensively characterized previously (Porter *et al.*, 2010). Mice were euthanized at 4 and 24 h following pulmonary exposure. Serum was collected and the left lung lobe was ligated and removed to preserve for MMP-9 protein determinations. Bronchoalveolar lavage (BAL) was performed on the right lung lobes and the first lavage supernatant was assessed for lactate dehydrogenase (LDH) activity, albumin concentration, and MMP-9 levels.

Fractionation and mass spectrometry

Serum was first processed through a 0.1 μm Ultrafree-MC filtration unit (EMDMillipore, Billerica, Massachusetts) per manufacturer instructions. The clarified serum (100 μl) was then processed through a precleaned Amicon Ultra-0.5 centrifugal filter with Ultracel-30 membrane (EMDMillipore) per manufacturer instructions at 10 °C. Filtered sera (n = 5 per 0, 10, 40 μg MWCNT-7 groups) were prepared for liquid chromatography—tandem mass spectrometry (LC/MSMS). Samples (32 μl) were acidified with 8 μl of 1% formic acid, with 4 μl loaded onto a Symmetry C18 reversed-phase trap column using a NanoAcquity UPLC (Waters, Milford, Massachusetts). Separation was performed with a 150 mm × 75 μm HSS T3 reversed-phase capillary column at 55 °C online with a nanoelectrospray equipped Synapt G2 HDMS tandem mass spectrometer (Waters). Separation and data-independent mass spectrometric analysis with ion mobility was performed as described previously (Fuller *et al.*, 2012; Ottens *et al.*, 2014) with the modifications that gradient elution was performed from 2% to 42% acetonitrile in water (formic-acid modified) and spectra were collected between 200 and 1800 m/z, with a collision

energy ramp from 32 to 52 eV. All spectra were post-processed employing PLGS ion processing software (Waters). Generated ion tables were clustered and aligned by retention time (± 1.0 min), drift time (± 4 bins), and ion mass (MH+, ± 12 ppm) using Isoquant software (v1.6 beta) (Distler *et al.*, 2014; Kuharev *et al.*, 2014). Results were filtered to include only reproducible ion events (observed in 4 or more biological replicates per group). Ion mass tables per group were then evaluated and compared using histogram analysis with a minimum size of 500 Da.

Cell culture

Mouse cerebrovascular endothelial cells (mCECs) were obtained from a commercial vendor (Cell Biologics) and maintained according to manufacturer's recommendations at 37° and 5% CO_2 with complete endothelial cell medium supplemented with 10% Fetal Bovine Serum. All experiments were performed between passages 3 and 8. Assays were batched by exposure to enhance consistency and comparability across samples.

Spin trapping of MCEC-generated NO using electron paramagnetic resonance

To test the generation of NO, serum from control or MWCNT-7-treated mice (4 h post) was added to the mCECs at a ratio of 1:9 (10%) with basal endothelial cell medium. Electron paramagnetic resonance (EPR) spectroscopy was conducted according to previously described methods with some modifications (Paffett *et al.*, 2015). Following serum treatment, mCECs were incubated with the iron-chelate NO-spin trap Fe^{2+}-di(N-methyl-D-glutaminedithiocarbamate) ($Fe^{2+}(MGD)_2$; 1mM, final concentration) for 5 min. The iron-chelator $Fe^{2+}(MGD)_2$ was freshly prepared by mixing a stock solution of ferrous sulfate ($FeSO_4$; 20 mM, dissolved in deionized water under N_2) and an equal volume of sodium N-methyl-D-glucamine dithiocarbamate (NaMGD; 100 mM, dissolved in deionized water under N_2) to give a molar ratio of 1:5, respectively, prior to each experiment. Following the incubation period, the incubation medium (400 µl) containing spin trapped NO was immediately transferred into custom-made gas permeable Teflon tubing (Zeus Industries, Raritan, New Jersey), folded 4 times, and inserted into a quartz EPR tube open at each end. The quartz EPR tube was inserted within the cavity of a Bruker EleXsys E540 X-band EPR spectrometer (Billerica, Massachusetts) operating at 9.8 GHz and 100 kHz field modulation and spectra was recorded after spectrometer tuning at room temperature. The EPR spectrum of spin trapped-NO were acquired from untreated mCECs with a scan time of 40 s, and 10 scans were obtained and averaged to produce significant signal-to-noise ratio. EPR measurements from mCECs stimulated with 2 mM adenosine triphosphate (ATP) to induce NO release were performed under the same conditions. Instrument settings were as follows: magnetic field, 3440 G; scan range, 100 G; microwave power, 21 mW; modulation frequency, 100 kHz; modulation amplitude, 1.0 G; time constant, 20 ms. The EPR spectra were collected, stored, and manipulated using the Bruker Software Xepr (Billerica, Massachusetts). NO levels were quantified and peak-to-peak measurements were taken and expressed in relative units.mCECs were grown to confluence on 6-well plates and incubated for 4 h with 10% serum from MWCNT-exposed mice. Following serum treatment, mCECs were incubated with $Fe^{2+}(MGD)_2$. Following application of the trap, a supernatant sample was isolated and NO was measured to assess a baseline reading. NO generation at baseline was negligible. Endothelial cells were subsequently stimulated with 2 mM ATP for 5 min, followed by measurement of NO in a second supernatant sample.

Ex vivo vascular function using myography

Rings from the thoracic aorta were isolated and cleaned of connective tissue. Segments of aorta (2 mm length) were mounted in a 4-chamber myograph (610M; Danish Myo Technology A/S, Aarhus, Denmark). Vessels were submerged in physiological saline solution (composition in millimolar: 119.0 NaCl, 25.0 $NaHCO_3$, 5.5 glucose, 4.7 KCl, 1.2 $MgSO_4$, 1.2 KH_2PO_4, 0.025 EDTA, 2.5 $CaCl_2$) bubbled at 37 °C with 21% O_2–5% CO_2 balance N_2 and left to equilibrate for 30 min. Tension was applied in 2 mN stepwise increments over 30 min to an optimal passive tension of 9 mN. Preliminary experiments showed that this tension produced optimal contraction and relaxation responses. Data from force transducers were processed by a MacLab/4e A-DI converter displayed through LabChart software (AD Instruments).

Vessel viability was confirmed by a contractile response to the addition of potassium containing physiological salt solution (KPSS in millimolar: 64.9 NaCl, 25.0 $NaHCO_3$, 5.5 glucose, 58.9 KCl, 1.2 $MgSO_4$, 1.2 KH_2PO_4, 0.025 EDTA, 2.5 $CaCl_2$) repeated twice. Aortic rings isolated from naïve C57BL/6J or CD36-null mice were mounted in a myograph and challenged twice with KPSS as described above. After a 30-min equilibration period, vessels were incubated with 1% serum that was collected from mice exposed to dispersion media or MWCNT. Because the addition of serum induced contraction of aortic rings, the cumulative concentration-response curves to ACh (10^{-9} to 10^{-4}) were acquired only after the response to serum had stabilized.

MMP protein levels in lung

Lung lavage fluid and whole lung homogenates were assayed for MMP-2 and MMP-9 protein concentrations using enzyme-linked immunosorbent assays according to manufacturer's instructions (Boster, Pleasanton, California).

Statistics

Myographic studies were compared with a 2-way analysis of variance considering exposure and acetylcholine (ACh) concentration as the 2 factors, and *post hoc* comparisons at specific ACh concentrations were conducted using Tukey's multiple comparison *post hoc* testing (GraphPad Prism, v 6.0). Other comparisons were conducted with a standard 1-way analysis of variance with Dunnett's *post hoc* test for multiple comparisons.

RESULTS

Multiwalled Carbon Nanotube Exposure Results in Lung Cytotoxicity and Permeability Changes

MWCNT-7 used in this study have been previously characterized (Porter *et al.*, 2010). The average diameter was 49 nm with a mean length of 3.86 µm (geometric standard deviation = 1.94; Figs. 1A and B). Purity was >99% carbon. Exposure to MWCNT-7 resulted in a dose-dependent increase in BAL LDH activity at the 4 h time point, which also remained elevated at the 24 h time point. The 40 µg dose approximately doubled LDH levels compared with controls at both time points, with the 10 µg dose resulting in a 50% increase at both time points (Figure 1C). There was no significant difference in albumin levels between groups at the 4 h time point; however, both the 10 and 40 µg

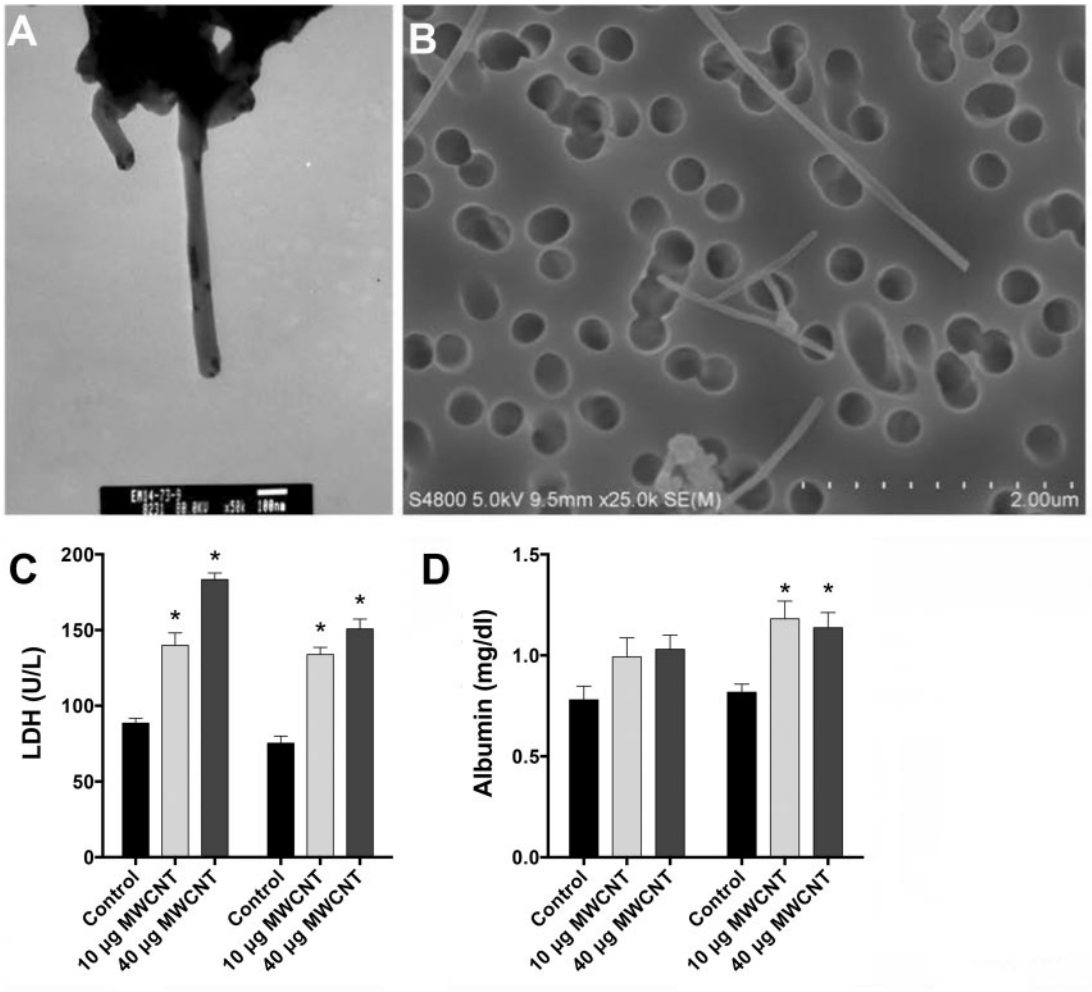

FIG. 1. A and B, MWCNT-7 imaging by electron microscopy demonstrates the relative size and adequacy of dispersion. C and D, Markers of injury in the lung lavage, LDH and albumin levels, were increased following exposure (*P < .05 vs DM by ANOVA, N = 4–8 per group). MWCNT: multiwalled carbon nanotubes.

doses showed elevated albumin at the 24 h time point when compared with controls (Figure 1D).

Serum From MWCNT-Exposed Mice Decreases Endothelial NO Generation In Vitro

The supernatant of serum-treated endothelial cells, when treated with ATP and the NO spin-trap MGD, afforded a strong signal detectable by EPR spectroscopy (Figure 2A). Baseline measurements of unstimulated endothelial cells resulted in negligible amounts of NO production between groups treated with exposed or control serum. In ATP-stimulated cells, however, serum from MWCNT-7-exposed mice decreased NO bioavailability by 30% when compared with cells incubated with serum from DM control mice (Figure 2B).

These results led us to speculate that the serum from MWCNT-7-exposed mice was able to directly affect eNOS or that the serum had the capacity to "scavenge" produced NO. To address this question we applied an acellular assay, bypassing the contribution of eNOS. MGD in iron-free media was incubated with serum from MWCNT-exposed mice and the NO-donor spermine NONOate (1M) as in previous studies with serum from ozone-exposed rodents (Paffett *et al.*, 2015). However, serum from MWCNT-7-exposed mice had no effect on NO bioavailability when compared with serum from control mice (Figure 2C). These results suggested that serum from MWCNT-7-exposed mice diminishes eNOS generation of NO, rather than NO bioavailability.

Serum From MWCNT-7-Exposed Mice Diminishes Vasorelaxation Ex Vivo

We next examined the role that MWCNT exposure might have in a functional physiological system. We employed force-transduction myography with an isolated aortic ring preparation to test the serum bioactivity. Serum from both doses of MWCNT-7-exposed mice was able to significantly reduce ACh-induced relaxation (Figure 3). Interestingly, the serum from 10 µg-treated mice collected 4 h postexposure (Figure 3A) was more potent in terms of inhibiting relaxation than was serum from 40 µg-treated mice, with the lower dose reaching a maximum relaxation of only 13.6%, compared with 27.1% for the higher dose and 49.4% for vehicle controls. This effect persisted at least 24 h postexposure (Figure 3B), although more variability was noted. At 24 h post exposure, serum from both low and high dose groups similarly inhibited relaxation (26.9% and 28.5%, respectively), as compared with DM control serum.

In addition to ACh responses, we assessed whether the initial contraction induced by serum treatment was similar between groups. Maximum vessel constriction induced by serum

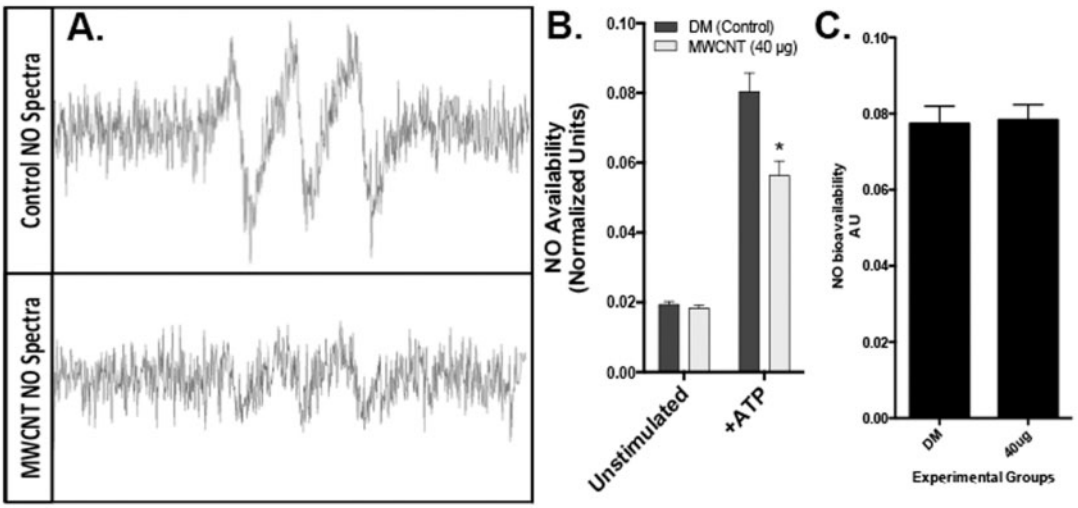

FIG. 2. Effects of serum from MWCNT-7-exposed mice on NO generation and bioavailabilty. A, Representative EPR spectra from endothelial cells incubated with control serum and serum from MWCNT-7-exposed mice. B, Unstimulated endothelial cells exhibited minimal baseline levels of detectable NO, which was not different when incubated with serum from DM (control) or MWCNT-7-treated mice. However, when stimulated by ATP, endothelial cells incubated with control serum demonstrated a significantly greater capacity to generate NO than cells treated with serum from MWCNT-7-exposed mice (*$P < .05$, $N = 3$ per group). C, In an acellular assay, levels of NO in iron-free media containing a known concentration of the NO donor, spermine NONOate, were not different in the presence of serum from control or MWCNT-7-treated mice. NO: nitric oxide; EPR: electron paramagnetic resonance.

was measured and normalized to a KPSS response. There were no differences between control and MWCNT doses at 4 h with complete serum (Figure 3A right panel). However, serum obtained 24 h following MWCNT exposure did induce a modest but significantly higher average constriction in the 40 μg group (101% vs 80% for the low dose and 87% for the control; Figure 3B right panel).

Impact of Serum Fractionation on Vasorelaxation Responses

As an initial attempt to understand how serum bioactivity is driven by altered biochemistry and to exclude a direct nanomaterial effect on vasorelaxation, the serum was filtered to resolve smaller components (<10 kDa) for aortic ring treatments. Notably, the filtered serum allowed for greater overall relaxation to ACh compared with whole serum, with an average relaxation of 77.39% for aortic rings incubated with filtered serum from DM-treated mice. In the 4 h post-exposure samples, the <10 kDa biomolecules induced a prominent anti-relaxation effect of serum from both doses of MWCNT-7-exposed mice, although the specific enhanced potency of the 10 μg dose was no longer observed (Figure 4A). The anti-relaxant effect of filtered serum components from MWCNT-7-treated mice was largely abolished in the 24 h postexposure serum (Figure 4B), suggesting that the <10 kDa biomolecules may have complexed with larger biomolecules or that larger biomolecules contribute to a persistent effect. There were no differences in initial contraction between control and MWCNT doses with 4 h filtered serum (removal of large, >10 kDa proteins), or with 24 h filtered serum (Figure 4A and B right panels, respectively).

We employed LC/MSMS analysis to confirm that the serum fraction consisted of biomolecules below 10 kDa (Figure 4C). Further, in comparing the <10 kDa serum fraction between treatment groups, we resolved differences in the mass distribution among doses, consistent with the observations of nonlinear dose effects. Importantly, findings with filtered sera demonstrate that bioactivity can be induced without any possibility of direct nanomaterial or leukocyte interaction with the endothelium.

Vascular CD36 Mediates Endothelial Dysfunction Induced by Serum from MWCNT-7-Exposed Mice

Aortas harvested from CD36-null mice were employed to determine if the scavenger-receptor mediated effects of serum from MWCNT-7-exposed mice were similar to previous findings with ozone and ambient PM. CD36-null aortic relaxation in response to ACh was not impacted by serum from MWCNT-7-exposed mice compared with serum from control mice (Figure 5). All 3 groups reached an average maximum relaxation of approximately 50% (comparable to wildtype [WT] vessels), with no discernible differences between the groups at either time point. These results denote that the bioactive compounds in the serum following MWCNT-7 exposure interact with CD36 to impair vasorelaxation.

Interestingly, however, serum from MWCNT-7-exposed mice applied to $CD36^{-/-}$ vessels was observed to induce a greater average contraction of 100% for the lower and 104% for the higher dose group at the 4 h mark compared with aortic rings treated with control serum (87%; Figure 5A right panel). By 24 h, the high dose group achieved a contraction of 101%, while the low dose was not different from controls (Figure 5B right panel). These findings contrast with the vasorelaxation data in that CD36 is not required to induce contraction due to MWCNT-induced, serum-borne components.

Serum From MMP-9 Deficient Mice Exhibits Reduced Vascular Bioactivity After MWCNT-7 Exposure

Lastly, we investigated the potential role of MMP-9 as a source of circulating ligands that are generated as a result of MWCNT-7 exposure. MMP-9 levels in WT mice treated with 10 and 40 μg MWCNT-7 were measured in the lung and BAL at the protein level. MMP-9 was up regulated in the BAL at both 10 and 40 μg doses at 4 h, and in the 40 μg dose at 24 h (Figure 6A and B). MMP-9 was also significantly upregulated in the lung lysate in

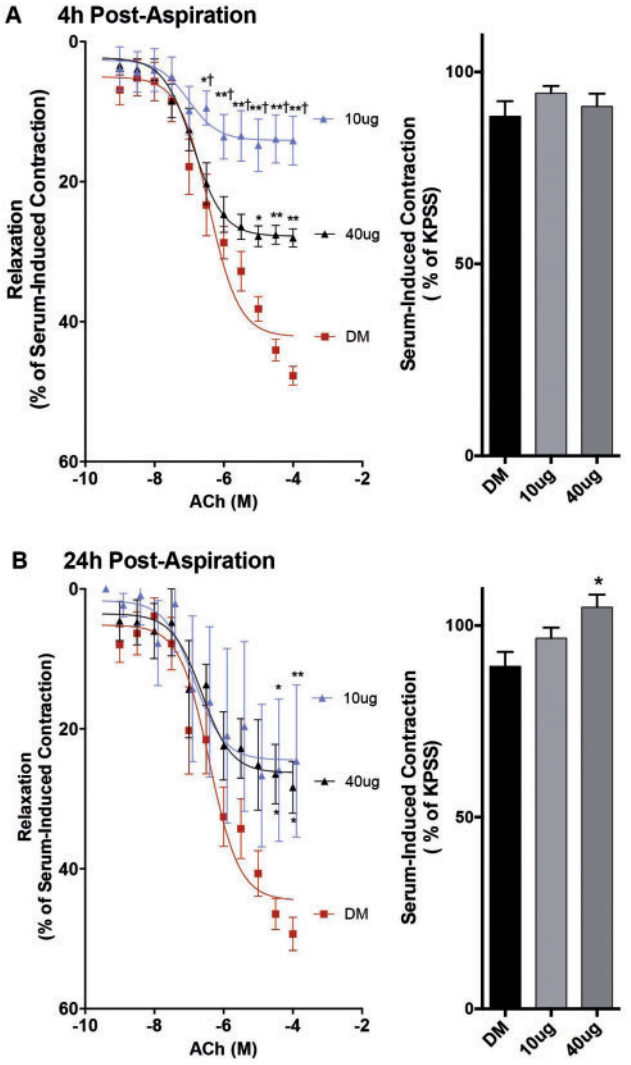

FIG. 3. A, Mouse serum obtained 4 h following MWCNT-7 treatment inhibited ACh-mediated vasorelaxation in aortic rings from untreated (naïve) mice (left) and maximum vessel constriction induced by serum (normalized to a KPSS response; right). Interestingly, the serum from low dose-treated mice was more potent than serum from high dose-treated mice. Asterisks indicates significant difference from control by 2-way ANOVA with Tukey's multiple comparison test (*$P < .05$, **$P < .001$), dagger represents significant difference between the 10 and 40 μg doses ($^{\dagger}P < .01$; $N = 10$ per group). B, Mouse serum obtained 24 h following MWCNT-7 treatment inhibited ACh-mediated vasorelaxation in aortic rings from untreated (naïve) mice (left), however the increased potency of the low dose exposure at 4 h was no longer observed. Maximum vessel constriction induced by serum (normalized to a KPSS response) is also shown (right of each relaxation curve). *Indicates significant difference from DM control by 2-way ANOVA (*$P < .05$, **$P < .01$; $N = 6-8$ per group). Ach: acetylcholine; KPSS: potassium containing physiological salt solution.

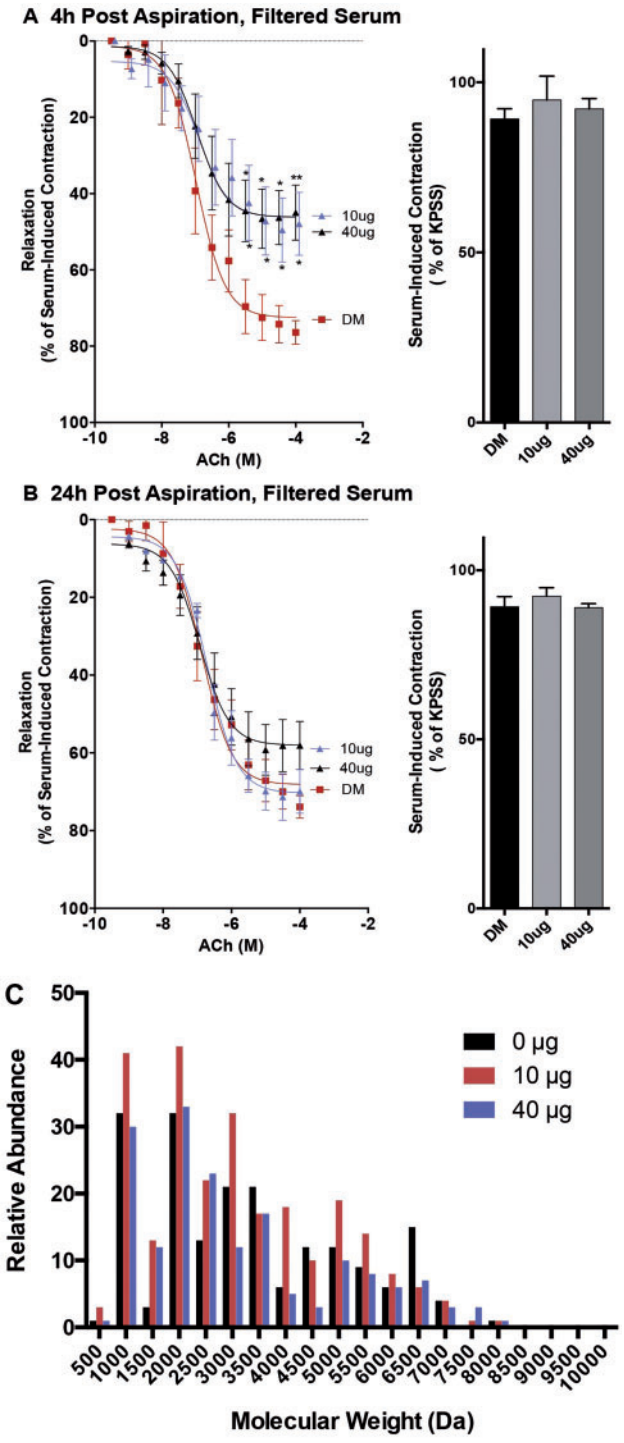

FIG. 4. A, Mouse serum obtained 4 h following MWCNT-7 treatment was filtered to remove all larger proteins, leaving only biomolecules <10 kDa. This filtered serum still inhibited ACh-mediated vasorelaxation in aortic rings from untreated (naïve) mice. Asterisks indicate significant difference from control by 2-way ANOVA with Tukey's multiple comparison test (*$P < 0.05$, **$P < .01$; $N = 5$ per group). B, Filtered mouse serum obtained 24 h following MWCNT-7 treatment did not affect ACh-mediated vasorelaxation in aortic rings from untreated mice ($N = 5$ per group). C, Mass spectroscopic analysis of numerous biomolecules ranging from 0.5 to 10 kDa remaining after filtration confirms the removal of large molecules in this bioactive fraction. Individual peaks are collected into bins of the histogram and separated by dose group for the 4 h posttreatment serum.

the 40 μg dose at 24 h (Figure 6D). In contrast, MMP-2 protein levels were unchanged in the lung lavage (Supplementary Figure 1).

Building on the finding of MWCNT-7-induced pulmonary MMP-9 expression, MMP-$9^{-/-}$ mice were exposed to MWCNT-7 and the bioactivity of the serum was tested for its ability to affect eNOS mediated vasorelaxation *ex vivo*. Deficiency of MMP-9 (Figure 7) appeared fully protective relative to WT outcomes (Figure 3). Pulmonary MWCNT-7 cytotoxicity, as measured by LDH activity in the bronchoalveolar lavage fluid (BALF), was similar between both WT and MMP-$9^{-/-}$ mice (Figure 7A). In

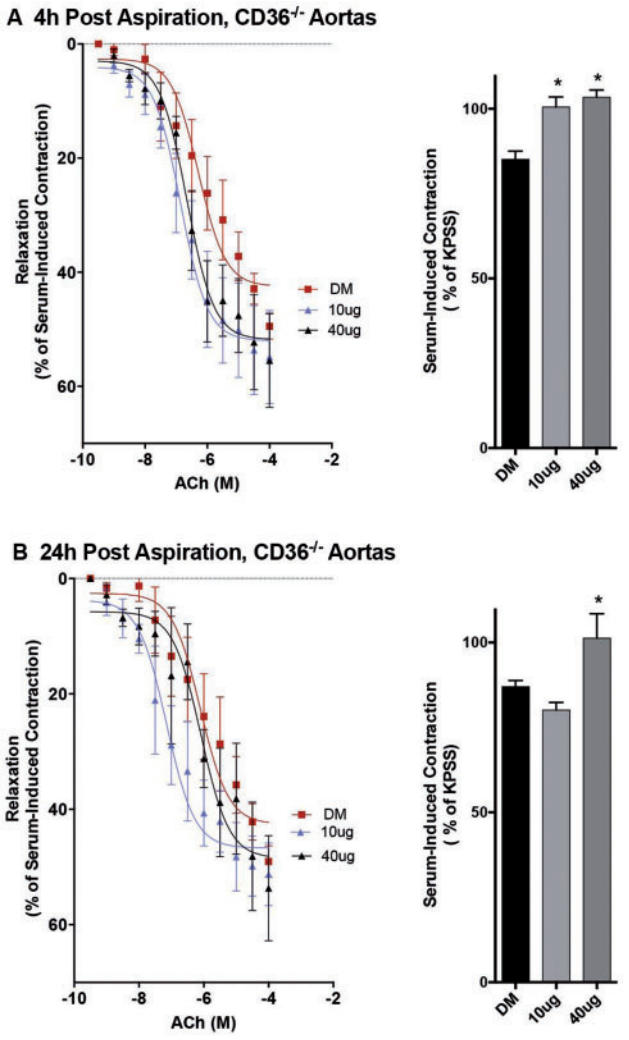

FIG. 5. A, Mouse serum obtained 4 h following MWCNT-7 treatment had no effect on ACh-mediated vasorelaxation in aortic rings from untreated CD36-null mice (N = 5 per group). Significant differences in the contractile response to the serum addition were noted for serum from MWCNT-7-treated mice. Asterisks indicate significant difference from control by ANOVA with Dunnett's multiple comparison test (*P <.05; n = 5 per group). B, Filtered mouse serum obtained 24 h following MWCNT-7 treatment had no effect on ACh-mediated vasorelaxation in aortic rings from untreated CD36-null mice (N = 4–5 per group). Significant differences in the contractile response to the serum addition were noted for serum from the 40 μg MWCNT-7-treated mice. Asterisks indicate significant difference from control by ANOVA with Dunnett's multiple comparison test (*P < .05; n = 5 per group).

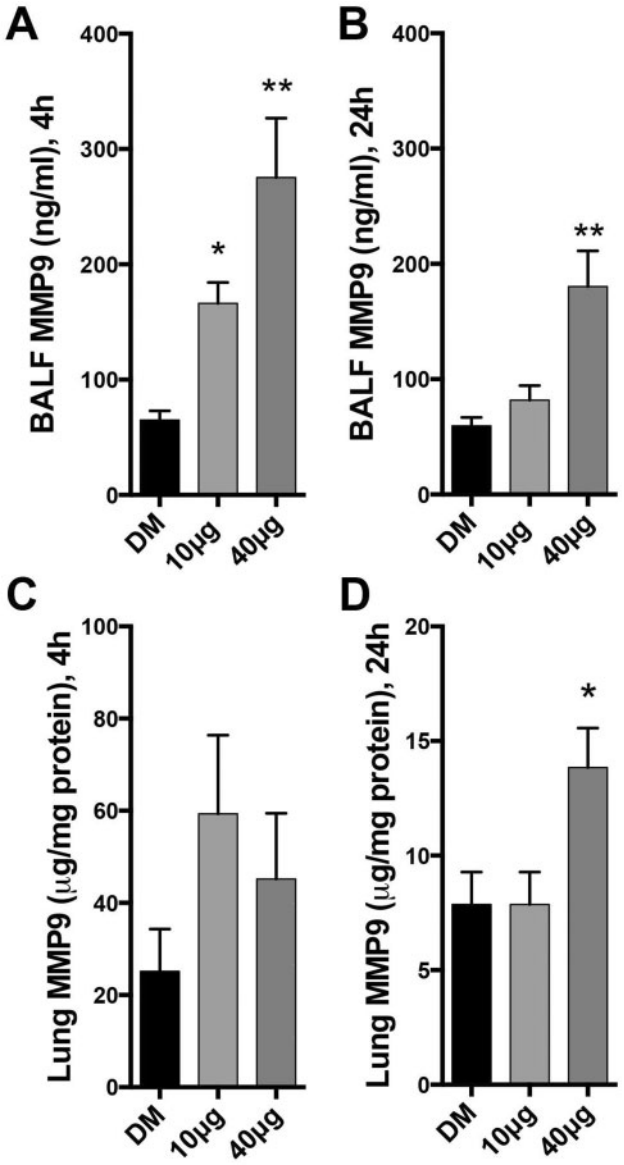

FIG. 6. MMP-9 protein levels in bronchoalveolar lavage (A and B) and whole lung lysates (C and D) from MWCNT-7-exposed mice. Asterisks indicate significant difference from control by ANOVA with Dunnett's multiple comparison test (*P < .05; **P < .01).

both dose groups, WT vessels treated with serum from MMP-$9^{-/-}$ mice achieved similar maximal relaxation compared with serum from DM-treated MMP-$9^{-/-}$ mice, with an average response of approximately 55% (Figure 7B). However, the dose-response curve revealed a significant right-shift in both dose groups relative to DM-control serum, which suggests that some residual bioactivity may be derived outside of MMP-9 activity. DM-control serum from the MMP-$9^{-/-}$ mice was actually more permissive of vasorelaxation that WT serum in this *ex vivo* assay, which further adds to the conjecture that MMP-9-derived degradation products may impair vascular function (Supplementary Figure 2). Serum-mediated constriction (Figure 7C) was unaltered between exposure groups in the MMP-$9^{-/-}$ animals. Collective maximal vasorelaxation outcomes for each permutation at the 4-h time point clearly show that pulmonary MWCNT-7 exposure leads to bioactivity in the serum that impairs vasorelaxation in a manner dependent on MMP-9 to generate the signal and CD36 to respond (Supplementary Figure 3).

DISCUSSION

In this study, we provide functional evidence for a mechanism by which MWCNT-7 exerts systemic endothelial dysfunction, which appears to be indirectly mediated by serum-borne components. Pulmonary exposure to MWCNT-7 led to the generation of bioactive factors in the serum that significantly impaired vascular function *ex vivo*. Furthermore, the principal components of the serum that confer abnormal vasorelaxation act through the vascular CD36 scavenger receptor and appear, at least acutely (4 h), to involve smaller biomolecules (<10 kDa)

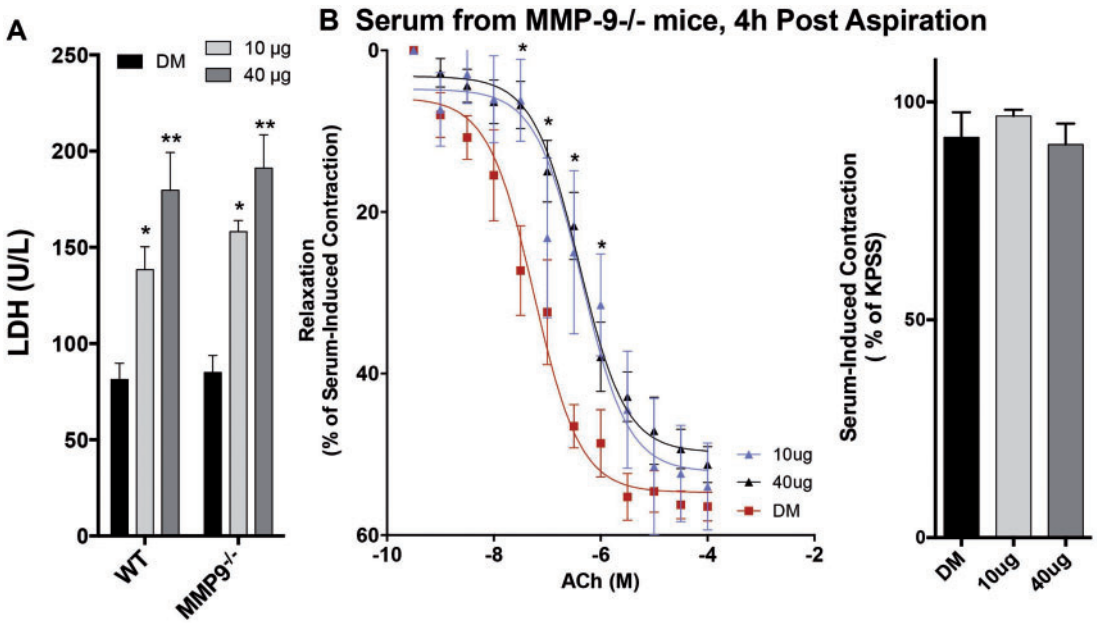

FIG. 7. A, MMP-$9^{-/-}$ mice exhibit similar degree of lung injury at 4 h post MWCNT-7 aspiration, as measured by LDH from the BALF. Asterisks indicate significant difference from control by 2-way ANOVA with Tukey's multiple comparison test (*P < .01; **P < .001). B, Serum from MMP-$9^{-/-}$ mice treated with 10 or 40 µg MWCNT-7 caused a modest right-shift effect on the concentration response to ACh-mediated vasorelaxation in WT vessels, compared with serum from the DM control mice, but did not reduce the overall magnitude of relaxation. Serum from the various groups exhibited a consistent contractile effect on all aortas. Asterisks indicate significant difference from control by 2-way ANOVA with Tukey's multiple comparison test (*P < .05; n = 5–6 per group).WT: wild type; MMP-9: matrix metalloproteinase-9; DM. dosing media.

released into circulation. The effects of MWCNT-7-induced serum biomolecules were not linearly associated with lung burden and may reflect induction of different biological responses at different doses. Within this study, we outline a plausible pathway by which ligands are derived from MMP-9 activity in the lung, access the circulation and interact with vascular CD36 receptors to reduced vasorelaxation. This overarching paradigm provides concrete mechanistic detail to theories of pulmonary "spillover" that explain the pathogenesis of extrapulmonary effects of inhaled particulates (Brook *et al.*, 2010; Van Eeden *et al.*, 2012), although the biological complexity with potentially numerous metalloproteinases and pattern recognition receptors involved must be considered. Importantly, the observed vascular effects with serum from mice exposed to MWCNT-7 by a pulmonary route resolves issues inherent to direct-application nanomaterial research with cells or organs, offering an alternative and more anatomically sound (or route-appropriate) approach to study mechanisms underlying the extrapulmonary toxicity of inhaled particulates.

How serum from MWCNT-7-exposed mice exerts its effects on vascular relaxation presumably involves impairment of eNOS and NO generation. Inhalation of pollutants such as diesel emissions can lead to uncoupling of eNOS and similar loss of dilatory function (Cherng *et al.*, 2011; Knuckles *et al.*, 2008). Nurkiewicz *et al.* (2009) found that TiO_2 nanoparticles could directly scavenge NO, an effect that was eliminated in the presence of antioxidants. We recently observed that serum from ozone-exposed rats exhibited diminished serum levels of nitrites and nitrates, and there was some evidence for increased nitrosothiol formation in serum, suggesting that NO scavenging may occur (Paffett *et al.*, 2015). In this study, however, serum from MWCNT-7-exposed mice inhibited aortic vasorelaxation and endothelial cell generation of NO, but did not scavenge spermine NONOate-donated NO. The outcomes from cell culture and isolated aortic rings suggest that a ligand-receptor interaction, and resultant intracellular signaling, mediated a loss of eNOS activity, and diminished vasorelaxation.

One potential mechanism to explain how serum from MWCNT-7-exposed mice could impair eNOS is through the generation of CD36-interacting ligands, such as oxidized lipids or thrombospondin repeat-containing peptides, which have both been shown to impair vasorelaxation (Bauer *et al.*, 2010; Matsuda *et al.*, 1993; Silverstein and Febbraio, 2009; Uittenbogaard *et al.*, 2000). Specific ligands to CD36 can adversely affect the lipid composition of caveole, interfering with eNOS and potentially causing eNOS to become uncoupled (Fleming *et al.*, 2005; Shaul, 2003; Wong *et al.*, 2011). The present data, combined with recent studies of ozone-induced endothelial dysfunction (Robertson *et al.*, 2013), implicate an important role for CD36 in mediating the loss of aortic vasorelaxation caused by serum from MWCNT-7-treated mice. Notably, vessel relaxation in CD36-null aortas was more robust than in WT aortas when treated with control serum. CD36 has been implicated as a key inflammatory mediator in response to PM exposure, an important component of the macrophage response to oxidized lipids (Rao *et al.*, 2014) and thus may have broader implications for extrapulmonary effects than just endothelial dysfunction (Robertson *et al.*, 2013).

We propose that an additional crucial step required for the induction of eNOS-compromising bioactivity in serum from MWCNT-7-exposed mice involves the activation of pulmonary MMP-9, leading to the generation of protein fragments that can affect biological activity. MMP-9 plays a major role in the degradation of extracellular matrix in a large spectrum of physiological and pathophysiological process (Bekes *et al.*, 2011). MMP-9 is secreted by a wide number of cell types including neutrophils, macrophages, and fibroblasts, creating the potential for a large amount of MMP-9 to be generated as a result of lung

injury. Exposures to gasoline engine emissions in mice led to system-wide changes in MMP-9 concentrations and activity, including induction within atherosclerotic plaques (Lund *et al.*, 2009). Furthermore, serum MMP-9 was found to be elevated in both mice and humans exposed to diesel emissions (Lund *et al.*, 2009). Pulmonary MMP-9 expression has also been associated with vanadium (Colin-Barenque *et al.*, 2008), a vanadium-laden particulate (Su et al., 2000), and metal fume (Palmer *et al.*, 2006) exposures. Few studies have examined the pathophysiological implications of MMP-9 activity in mediating pulmonary or extrapulmonary outcomes of inhaled particulates. Our study found that despite comparable acute (4-h) lung injury from MWCNT-7 exposure in WT and MMP-9$^{-/-}$ mice, MMP-9 deficiency resulted in diminished serum bioactivity after MWCNT-7 treatment compared with WT. Interestingly, serum from MMP-9 deficient mice treated with vehicle allowed for greater relaxation in aortic rings than did WT serum. MMP-9 has been shown to generate numerous vasoactive by-products from the degradation of extracellular matrix proteins, such as angiostatin (Cornelius *et al.*, 1998; Pozzi *et al.*, 2000), tumstatin (Hamano *et al.*, 2003), and β-dystroglycan (Agrawal *et al.*, 2006). MMP-9 may therefore be responsible for the generation of a number of vasoactive agents that help set baseline vascular tone.

Our study highlights the importance of pulmonary nanoparticle delivery in driving systemic vascular effects and the doses used in this study, based on numerous dosimetry analyses, represent an extreme but plausible scenario (Erdely *et al.*, 2013). It should be appreciated that more pronounced effects were achieved at lower depositions and a 1:100 dilution of serum from exposed mice nearly abolished vascular relaxation. Mice have a blood volume of approximately 2 ml, depending on their body weight. Even if all of the MWCNT-7 left the lungs and stayed in the bloodstream—a gross exaggeration—the MWCNT-7 concentration in serum would be approximately 5 μg/ml, which would then be further diluted in the vascular bath to a maximal theoretical (yet still improbably high) concentration of 50 ng/ml, a concentration far below what has been reported to induce endothelial cell toxicity *in vitro*. The rationale for this extreme estimation of dose lies in how pulmonary exposure to particulates leads to a clear systemic vascular toxicity that cannot be reproduced with direct exposures of particles to the vessels. Furthermore, filtration of serum which would exclude molecules >10 kDa and certainly any trace of MWCNT-7, did not entirely abrogate vascular effects. Studies employing an oral gavage of carbon black were unable to induce substantial vascular dysfunction in rats (Folkmann *et al.*, 2012), and studies using an intravenous injection of diesel exhaust particles, at similar concentrations to the current MWCNT-7 doses, in mice were unable to induce vascular dysfunction (Bai and van Eeden, 2013). The lack of biological effect in these alternate exposure routes serves to highlight the importance of the pulmonary exposure in the pathogenesis of vascular outcomes. It should be further noted that occupational exposure to carbon nanotubes at typical concentrations (approximately 10 μg/m^3) would require 19 years of exposure (5 days/week) in humans to achieve the proportional lung burden in our lowest concentration (Erdely *et al.*, 2013). While the present study is primarily designed to address the underlying pathways leading to systemic vascular effects following pulmonary exposures, it must be clear that safety assessment at these concentrations *in vivo*, and even more so *in vitro*, require thoughtful consideration of the extrapolation to relevant doses.

In conclusion, serum obtained from mice exposed to MWCNT-7 has the capacity to impair vasorelaxation in naïve aortic rings *ex vivo*, an effect that persisted at least 24 h after exposure. Notably, the low dose of 10 μg induced even greater serum bioactivity at the 4-h time point than did the 40 μg dose, which we believe may be related to a discordance in the profiles of circulating factors generated by varying doses. Results from the present study further highlight the role of smaller, <10 kDa biomolecules, in addition to larger species, which appear to be generated by MMP-9 and may collectively act through the scavenger receptor CD36 to reduce responsiveness to ACh. These data further support the concept that pulmonary reactions lead to a spillover of secondary mediators from the lungs into the systemic circulation. Future work will need to further elucidate, via fractionation studies, which portions/components of the serum exhibit biological activity, as well as peptide sequencing to provide further insight into the enzymatic origins of the circulating peptides. Additionally, the use of serum from exposed mice in *ex vivo* assays offers a novel, more anatomically sophisticated and even translational approach for studying the systemic impact of inhaled substances.

Supplementary Data

Supplementary data are available online at http://toxsci.oxfordjournals.org/.

FUNDING

This study was funded by grants from the National Institute of Environmental Health Sciences (R01 ES014639), National Institute for Occupational Safety and Health (R21 OH010495; NTRC, 939ZXFL, and 927ZKGW), National Heart Lung and Blood Institute (T32 HL007736), and the National Institutes of Health Center of Biomedical Research Excellence (P30GM103400).

ACKNOWLEDGMENTS

A.K.O. thanks S. Tenzer from U. Mainz for customized beta release of Isoquant software for ion alignment of unidentified ions. A.E. thanks Diane Schwegler-Berry for the electron microscopy images of the MWCNT-7.

REFERENCES

Agrawal, S., Anderson, P., Durbeej, M., van Rooijen, N., Ivars, F., Opdenakker, G., and Sorokin, L. M. (2006). Dystroglycan is selectively cleaved at the parenchymal basement membrane at sites of leukocyte extravasation in experimental autoimmune encephalomyelitis. *J. Exp. Med.* **203**, 1007–1019.

Aird, W. C. (2008). Endothelium in health and disease. *Pharmacol. Rep.* **60**, 139–143.

Alheid, U., Frolich, J. C., and Forstermann, U. (1987). Endothelium-derived relaxing factor from cultured human endothelial cells inhibits aggregation of human platelets. *Thromb. Res.* **47**, 561–571.

Bai, N., and van Eeden, S. F. (2013). Systemic and vascular effects of circulating diesel exhaust particulate matter. *Inhal. Toxicol.* **25**, 725–734.

Bai, N., Khazaei, M., van Eeden, S. F., and Laher, I. (2007). The pharmacology of particulate matter air pollution-induced cardiovascular dysfunction. *Pharmacol. Ther.* **113**, 16–29.

Bauer, E. M., Qin, Y., Miller, T. W., Bandle, R. W., Csanyi, G., Pagano, P. J., Bauer, P. M., Schnermann, J., Roberts, D. D., and

Isenberg, J. S. (2010). Thrombospondin-1 supports blood pressure by limiting eNOS activation and endothelial-dependent vasorelaxation. *Cardiovasc. Res.* **88**, 471–481.

Bekes, E. M., Schweighofer, B., Kupriyanova, T. A., Zajac, E., Ardi, V. C., Quigley, J. P., and Deryugina, E. I. (2011). Tumor-recruited neutrophils and neutrophil TIMP-free MMP-9 regulate coordinately the levels of tumor angiogenesis and efficiency of malignant cell intravasation. *Am. J. Pathol.* **179**, 1455–1470.

Brook, R. D., Rajagopalan, S., Pope, C. A., 3rd, Brook, J. R., Bhatnagar, A., Diez-Roux, A. V., Holguin, F., Hong, Y., Luepker, R. V., Mittleman, M. A., *et al.* (2010). Particulate matter air pollution and cardiovascular disease: An update to the scientific statement from the American Heart Association. *Circulation* **121**, 2331–2378. (/CIR.0b013e3181dbece1.

Cherng, T. W., Paffett, M. L., Jackson-Weaver, O., Campen, M. J., Walker, B. R., and Kanagy, N. L. (2011). Mechanisms of diesel-induced endothelial nitric oxide synthase dysfunction in coronary arterioles. *Environ. Health Perspect.* **119**, 98–103.

Colin-Barenque, L., Martinez-Hernandez, M. G., Baiza-Gutman, L. A., Avila-Costa, M. R., Ordonez-Librado, J. L., Bizarro-Nevares, P., Rodriguez-Lara, V., Pinon-Zarate, G., Rojas-Lemus, M., Mussali-Galante, P. *et al.* (2008). Matrix metalloproteinases 2 and 9 in central nervous system and their modification after vanadium inhalation. *J. Appl.Toxicol.* **28**, 718–723.

Cornelius, L. A., Nehring, L. C., Harding, E., Bolanowski, M., Welgus, H. G., Kobayashi, D. K., Pierce, R. A., and Shapiro, S. D. (1998). Matrix metalloproteinases generate angiostatin: Effects on neovascularization. *J. Immunol.* **161**, 6845–6852.

Dagouassat, M., Lanone, S., and Boczkowski, J. (2012). Interaction of matrix metalloproteinases with pulmonary pollutants. *Eur. Respir. J.* **39**, 1021–1032.

Distler, U., Kuharev, J., Navarro, P., Levin, Y., Schild, H., and Tenzer, S. (2014). Drift time-specific collision energies enable deep-coverage data-independent acquisition proteomics. *Nat. Methods* **11**, 167–170.

Erdely, A., Dahm, M., Chen, B. T., Zeidler-Erdely, P. C., Fernback, J. E., Birch, M. E., Evans, D. E., Kashon, M. L., Deddens, J. A., Hulderman, T., *et al.* (2013). Carbon nanotube dosimetry: From workplace exposure assessment to inhalation toxicology. *Part. Fibre. Toxicol.* **10**, 53.

Erdely, A., Hulderman, T., Salmen, R., Liston, A., Zeidler-Erdely, P. C., Schwegler-Berry, D., Castranova, V., Koyama, S., Kim, Y. A., Endo, M., *et al.* (2009). Cross-talk between lung and systemic circulation during carbon nanotube respiratory exposure. Potential biomarkers. *Nano. Lett.* **9**, 36–43.

Febbraio, M., Abumrad, N. A., Hajjar, D. P., Sharma, K., Cheng, W., Pearce, S. F., and Silverstein, R. L. (1999). A null mutation in murine CD36 reveals an important role in fatty acid and lipoprotein metabolism. *J. Biol. Chem.* **274**, 19055–19062.

Febbraio, M., Hajjar, D. P., and Silverstein, R. L. (2001). CD36: a class B scavenger receptor involved in angiogenesis, atherosclerosis, inflammation, and lipid metabolism. *J Clin Invest* **108**, 785–791.

Fleming, I., Mohamed, A., Galle, J., Turchanowa, L., Brandes, R. P., Fisslthaler, B., and Busse, R. (2005). Oxidized low-density lipoprotein increases superoxide production by endothelial nitric oxide synthase by inhibiting PKCalpha. *Cardiovasc. Res.* **65**, 897–906.

Folkmann, J. K., Vesterdal, L. K., Sheykhzade, M., Loft, S., and Moller, P. (2012). Endothelial dysfunction in normal and prediabetic rats with metabolic syndrome exposed by oral gavage to carbon black nanoparticles. *Toxicol. Sci.* **129**, 98–107.

Fuller, B. F., Cortes, D. F., Landis, M. K., Yohannes, H., Griffin, H. E., Stafflinger, J. E., Bowers, M. S., Lewis, M. H., Fox, M. A., and Ottens, A. K. (2012). Exposure of rats to environmental tobacco smoke during cerebellar development alters behavior and perturbs mitochondrial energetics. *Environ. Health Perspect.* **120**, 1684–1691.

Hamano, Y., Zeisberg, M., Sugimoto, H., Lively, J. C., Maeshima, Y., Yang, C., Hynes, R. O., Werb, Z., Sudhakar, A., and Kalluri, R. (2003). Physiological levels of tumstatin, a fragment of collagen IV alpha3 chain, are generated by MMP-9 proteolysis and suppress angiogenesis via alphaV beta3 integrin. *Cancer Cell* **3**, 589–601.

Harrison, D. G. (1994). Endothelial dysfunction in atherosclerosis. *Basic Res. Cardiol.* **89(Suppl 1)**, 87–102.

Kampfrath, T., Maiseyeu, A., Ying, Z., Shah, Z., Deiuliis, J. A., Xu, X., Kherada, N., Brook, R. D., Reddy, K. M., Padture, N. P., *et al.* (2011). Chronic fine particulate matter exposure induces systemic vascular dysfunction via NADPH oxidase and TLR4 pathways. *Circ. Res.* **108**, 716–726.

Knuckles, T. L., Lund, A. K., Lucas, S. N., and Campen, M. J. (2008). Diesel exhaust exposure enhances venoconstriction via uncoupling of eNOS. *Toxicol. Appl. Pharmacol.* **230**, 346–351.

Kubes, P., Suzuki, M., and Granger, D. N. (1991). Nitric oxide: An endogenous modulator of leukocyte adhesion. *Proc. Natl. Acad. Sci. U.S.A.* **88**, 4651–4655.

Kuharev, J., Navarro, P., Distler, U., Jahn, O., and Tenzer, S. (2014). In-depth evaluation of software tools for data-independent acquisition based label-free quantification. *Proteomics.* **14**, 2607–2613.

Li, Z., Hulderman, T., Salmen, R., Chapman, R., Leonard, S. S., Young, S. H., Shvedova, A., Luster, M. I., and Simeonova, P. P. (2007). Cardiovascular effects of pulmonary exposure to single-wall carbon nanotubes. *Environ. Health Perspect.* **115**, 377–382.

Lund, A. K., Lucero, J., Harman, M., Madden, M. C., McDonald, J. D., Seagrave, J. C., and Campen, M. J. (2011). The oxidized low-density lipoprotein receptor mediates vascular effects of inhaled vehicle emissions. *Am. J. Respir. Crit. Care Med.* **184**, 82–91.

Lund, A. K., Lucero, J., Lucas, S., Madden, M. C., McDonald, J. D., Seagrave, J. C., Knuckles, T. L., and Campen, M. J. (2009). Vehicular emissions induce vascular MMP-9 expression and activity associated with endothelin-1-mediated pathways. *Arterioscler. Thromb. Vasc. Biol.* **29**, 511–517.

Matsuda, Y., Hirata, K., Inoue, N., Suematsu, M., Kawashima, S., Akita, H., and Yokoyama, M. (1993). High density lipoprotein reverses inhibitory effect of oxidized low density lipoprotein on endothelium-dependent arterial relaxation. *Circ. Res.* **72**, 1103–1109.

Mercer, R. R., Scabilloni, J. F., Hubbs, A. F., Wang, L., Battelli, L. A., McKinney, W., Castranova, V., and Porter, D. W. (2013). Extrapulmonary transport of MWCNT following inhalation exposure. *Part Fibre Toxicol.* **10**, 38.

Nunokawa, Y., and Tanaka, S. (1992). Interferon-gamma inhibits proliferation of rat vascular smooth muscle cells by nitric oxide generation. *Biochem. Biophys. Res. Commun.* **188**, 409–415.

Nurkiewicz, T. R., Porter, D. W., Hubbs, A. F., Cumpston, J. L., Chen, B. T., Frazer, D. G., and Castranova, V. (2008). Nanoparticle inhalation augments particle-dependent systemic microvascular dysfunction. *Part Fibre Toxicol.* **5**, 1.

Nurkiewicz, T. R., Porter, D. W., Hubbs, A. F., Stone, S., Chen, B. T., Frazer, D. G., Boegehold, M. A., and Castranova, V. (2009).

Pulmonary nanoparticle exposure disrupts systemic microvascular nitric oxide signaling. *Toxicol. Sci.* **110**, 191–203.

Ottens, A. K., Stafflinger, J. E., Griffin, H. E., Kunz, R. D., Cifu, D. X., and Niemeier, J. P. (2014). Post-acute brain injury urinary signature: A new resource for molecular diagnostics. *J. Neurotrauma* **31**, 782–788.

Paffett, M. L., Zychowski, K. E., Sheppard, L., Robertson, S., Weaver, J. M., Lucas, S. N., and Campen, M. J. (2015). Ozone inhalation impairs coronary artery dilation via intracellular oxidative stress: Evidence for serum-borne factors as drivers of systemic toxicity. *Toxicol. Sci.* **146**, 244–253.

Palmer, K. T., McNeill Love, R. M., Poole, J. R., Coggon, D., Frew, A. J., Linaker, C. H., and Shute, J. K. (2006). Inflammatory responses to the occupational inhalation of metal fume. *Eur. Respir. J.* **27**, 366–373.

Porter, D. W., Hubbs, A. F., Mercer, R. R., Wu, N., Wolfarth, M. G., Sriram, K., Leonard, S., Battelli, L., Schwegler-Berry, D., Friend, S., *et al.* (2010). Mouse pulmonary dose- and time course-responses induced by exposure to multi-walled carbon nanotubes. *Toxicology* **269**, 136–147.

Pozzi, A., Moberg, P. E., Miles, L. A., Wagner, S., Soloway, P., and Gardner, H. A. (2000). Elevated matrix metalloprotease and angiostatin levels in integrin alpha 1 knockout mice cause reduced tumor vascularization. *Proc. Natl. Acad. Sci. U.S.A.* **97**, 2202–2207.

Rao, X., Zhong, J., Maiseyeu, A., Gopalakrishnan, B., Villamena, F. A., Chen, L. C., Harkema, J. R., Sun, Q., and Rajagopalan, S. (2014). CD36-dependent 7-ketocholesterol accumulation in macrophages mediates progression of atherosclerosis in response to chronic air pollution exposure. *Circ. Res.* **115**, 770–780.

Robertson, S., Colombo, E. S., Lucas, S. N., Hall, P. R., Febbraio, M., Paffett, M. L., and Campen, M. J. (2013). CD36 mediates endothelial dysfunction downstream of circulating factors induced by O3 exposure. *Toxicol. Sci.* **134**, 304–311.

Sawada, H., Saito, Y., and Noguchi, N. (2012). Enhanced CD36 expression changes the role of Nrf2 activation from anti-atherogenic to pro-atherogenic in apoE-deficient mice. *Atherosclerosis* **225**, 83–90.

Shaul, P. W. (2003). Endothelial nitric oxide synthase, caveolae and the development of atherosclerosis. *J. Physiol.* **547**, 21–33.

Silverstein, R. L., and Febbraio, M. (2009). CD36, a scavenger receptor involved in immunity, metabolism, angiogenesis, and behavior. *Sci. Signal.* **2**, re3.

Su, W. Y., Jaskot, R. H., and Dreher, K. L. (2000). Particulate matter induction of pulmonary gelatinase A, gelatinase B, and tissue inhibitor of metalloproteinase expression. *Inhal. Toxicol.* **12(Suppl 2)**, 105-119.

Sun, Q., Wang, A., Jin, X., Natanzon, A., Duquaine, D., Brook, R. D., Aguinaldo, J. G., Fayad, Z. A., Fuster, V., Lippmann, M., *et al.* (2005). Long-term air pollution exposure and acceleration of atherosclerosis and vascular inflammation in an animal model. *Jama* **294**, 3003–3010.

Uittenbogaard, A., Shaul, P. W., Yuhanna, I. S., Blair, A., and Smart, E. J. (2000). High density lipoprotein prevents oxidized low density lipoprotein-induced inhibition of endothelial nitric-oxide synthase localization and activation in caveolae. *J. Biol. Chem.* **275**, 11278–11283.

Van Eeden, S., Leipsic, J., Paul Man, S. F., and Sin, D. D. (2012). The relationship between lung inflammation and cardiovascular disease. *Am. J. Respir. Crit. Care Med.* **186**, 11–16.

Wang, W., Deng, M., Liu, X., Ai, W., Tang, Q., and Hu, J. (2011). TLR4 activation induces nontolerant inflammatory response in endothelial cells. *Inflammation* **34**, 509–518.

Wong, W. T., Ng, C. H., Tsang, S. Y., Huang, Y., and Chen, Z. Y. (2011). Relative contribution of individual oxidized components in ox-LDL to inhibition on endothelium-dependent relaxation in rat aorta. *Nutr. Metab. Cardiovasc. Dis.* **21**, 157–164.